Structural Effects of Sulfur-Containing Functional Groups on Apatite Formation on Ca2+-Modified Copolymers in a Simulated Body Environment

ACS OMEGA

Article

Cite This: ACS Omega 2018, 3, 5627−5633

Structural Effects of Sulfur-Containing Functional Groups on Apatite Formation on Ca^{2+}-Modified Copolymers in a Simulated Body Environment

Ryo Hamai,[†] Yuki Shirosaki,[‡] and Toshiki Miyazaki*[,†]

[†]Graduate School of Life Science and Systems Engineering, Kyushu Institute of Technology, 2-4, Hibikino, Wakamatsu-ku, Kitakyushu 808-0196, Japan

[‡]Faculty of Engineering, Kyushu Institute of Technology, 1-1, Sensui-cho, Tobata-ku, Kitakyushu 804-8550, Japan

ABSTRACT: Chemical modification with specific functional groups has been the conventional method to develop bone-bonding bioactive organic−inorganic hybrids. These materials are attractive as bone substitutes because they are flexible and have a Young's modulus similar to natural bone. Immobilization of sulfonic acid groups ($-SO_3H$) onto the polymer chain is expected to produce such hybrids because these groups induce apatite formation in a simulated body fluid (SBF) and enhance the activity of osteoblast-like cells. Sulfinic acid groups ($-SO_2H$), which are derivatives of $-SO_3H$, can also induce apatite nucleation. However, the structural effects of such sulfur-containing functional groups on apatite formation have not been elucidated. In the present study, apatite formation on Ca^{2+}-modified copolymers containing $-SO_2H$ or $-SO_3H$ was investigated in a simulated body environment. The copolymer containing Ca^{2+} and $-SO_3H$ promoted Ca^{2+} release into the SBF and formed apatite faster (1 day) than the copolymer containing Ca^{2+} and $-SO_2H$ (14 days). In contrast, when they were not modified with Ca^{2+}, the copolymer containing only $-SO_2H$ deposited the apatite faster (7 days) than that containing only $-SO_3H$ (>7 days) in the solution with Ca^{2+} concentration 1.5 times that of SBF. The former adsorbed larger amounts of Ca^{2+} than the latter. The measured stability constant of the complex indicated that the interaction of $-SO_2^-\cdots Ca^{2+}$ was more stable than that of $-SO_3^-\cdots Ca^{2+}$. It was found that both the release and adsorption of Ca^{2+} governed by the stability played an important role in induction of the apatite formation and that the apatite-forming ability of sulfur-containing functional groups drastically changed by the coexistence of Ca^{2+}.

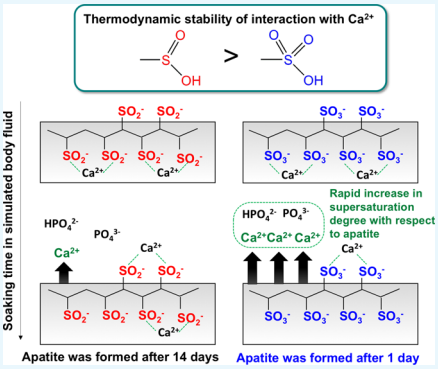

1. INTRODUCTION

Modifying with specific functional groups on the surface of implant materials to repair bone defects provides the implants with bone-bonding ability (i.e., bioactivity). Bone bonding is required for the longevity of the implant. Hench first showed that Bioglass bonds to the living bone without a foreign body reaction.[1] Subsequently, the glass ceramic A-W[2] and sintered hydroxyapatite[3,4] were developed as bioactive ceramics. When glass-based bioactive materials are implanted, the formation of low crystalline apatite induced by the surface Si−OH group and the release of Ca^{2+} is an important factor in their bonding to the living bone.[5]

Research has revealed that functional groups other than Si−OH allow the bonelike apatite formation on the material surface. Ti−OH,[6] Zr−OH,[7] Ta−OH,[8] carboxyl ($-COOH$),[9] phosphate ($-PO_4H_2$),[9] and sulfonate ($-SO_3H$)[10] groups induced heterogeneous nucleation of apatite in a simulated body fluid (SBF). SBF contains inorganic ions similar to those found in human blood plasma but does not contain the proteins.[11,12] Modifications of these functional groups have been used to fabricate bioactive metals,[13,14] organic−inorganic hybrids,[15,16] and polymer materials.[17] In particular, bioactive organic−inorganic hybrids and organic polymers are expected to be good bone substitutes as they can form into a defect shape and have a Young's modulus similar to the living bone.

To improve the biological compatibility of the hybrids and polymers, the effects of sulfonic acid group modification on apatite formation in SBF and activity of osteoblast-like cells on the surface have been examined. Miyazaki et al. created organic−inorganic hybrids consisting of poly[vinylsulfonic acid-*co*-2-hydoxyethyl methacrylate (HEMA)] and Ca^{2+}.[18] These hybrids formed apatite within 7 days in SBF and exhibited plastic deformation under mechanical property tests. Chaterji and Gemeinhart demonstrated that the increased sulfate group content in the poly(sulfopropyl acrylate-*co*-acrylamide) hydrogel improved the adhesion and proliferation of MG-63 osteoblast-like cells as a result of increased serum protein uptake.[19] Modification by plasma treatment also increased the activity of the osteoblasts on the scaffold because it allowed vitronection adsorption.[20] Therefore, incorporating sulfonic acid groups is potentially a way to prepare bioactive flexible materials.

Received: April 10, 2018
Accepted: May 15, 2018
Published: May 25, 2018

DOI: 10.1021/acsomega.8b00694
ACS Omega 2018, 3, 5627−5633

We previously reported the apatite-forming ability of copolymers modified with Ca^{2+} and the sulfinic acid ($-SO_2H$) group in SBF.[21] The copolymers formed apatite, and its morphology was significantly different by the existence of $-SO_2H$. These results mean that the $-SO_2H$ group also induced heterogeneous nucleation of the apatite in SBF. Although both $-SO_3H$ and $-SO_2H$ consist of the same elements, the number of bonding oxygen atoms in the structure is different. It is assumed that the structural differences affect the stability of the interaction with Ca^{2+} because the large number of oxygen atoms leads to stable ionized acidic functional groups because of the delocalization of the negative charge.[22] In fact, our previous research revealed that the stability of the interaction between the Ca^{2+} and $-PO_3H_2$ groups significantly changed the apatite-forming behavior of the Ca^{2+}-modified copolymers in SBF, depending on the chemical structure of the phosphate.[23] However, the structural effects of sulfur-containing acidic functional groups on the apatite-forming ability of the copolymers remain unclear.

In this study, we prepared copolymers consisting of Ca^{2+} and an organic matrix modified with $-SO_3H$ or $-SO_2H$ groups using sodium 4-vinylbenzenesulfonate ($NaVBSO_3$) or sodium 4-vinylbenzenesulfinate ($NaVBSO_2$) and HEMA. The mineralization behavior on the surface of hybrids was examined to determine the structural effects using analytical and surface chemistry techniques.

2. RESULTS

Figure 1 shows the Fourier transform infrared (FT-IR) spectra of different copolymer specimens before being soaked in the

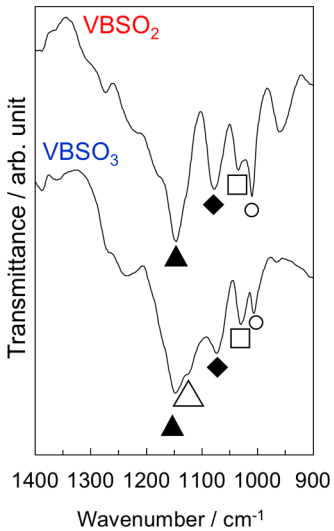

Figure 1. FT-IR spectra of the different copolymer specimens before being soaked in the $CaCl_2$ solution (▲: $\gamma(CH_3)$ or $\tau(OH)$ of HEMA; △: asymmetric stretching of O═S═O; ◆: ν(O−C) alcohol of HEMA; □: S═O bond of $VBSO_2$; ○: C−H bond of in-plane $VBSO_3$ and $VBSO_2$ deformation; ν is stretching, γ is rocking, and τ is torsion).

$CaCl_2$ solution. The HEMA peak in both spectra was observed at 1072 cm^{-1}, which was attributed to stretching vibration of the O−C bond for alcohol.[24] In addition, peaks corresponding to the vibration of CH_3 and torsion of the OH groups of HEMA were observed at 1146−1148 cm^{-1}. For both specimens, in-plane deformation vibrations of C−H and stretching vibration of S═O bonds were observed at 1030 and 1008 cm^{-1},[25] respectively. They were derived from both types of monomer-containing sulfur. $VBSO_3$ displayed a peak corresponding to the antisymmetric stretching vibration of O═S═O at 1122 cm^{-1},[26] but $VBSO_2$ did not.

Figure 2 shows the Ca and sulfur-containing acidic functional group content in the different specimens. $VBSO_2$ and $VBSO_3$

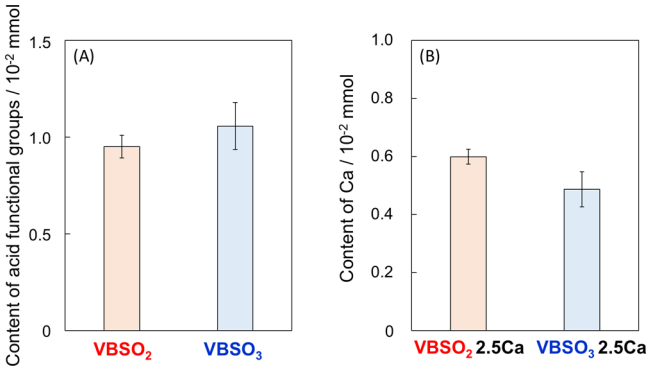

Figure 2. Content of (A) sulfur-containing acidic functional groups and (B) Ca in the specimens (n = 3).

contained nearly equivalent levels of each group. However, the content of Ca in $VBSO_3$ 2.5Ca was slightly lower than in $VBSO_2$ 2.5Ca. Figure 3 shows the change in Ca concentration

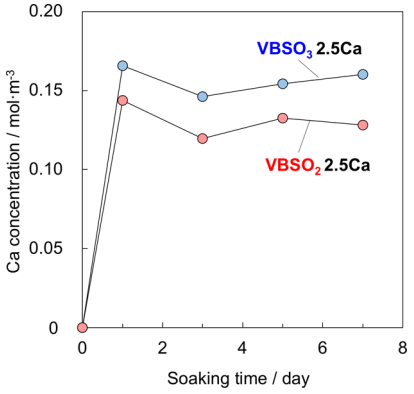

Figure 3. Change in Ca concentration in the Tris−NaCl buffer after soaking the different copolymer specimens for various time intervals.

in the tris(hydroxymethyl)aminomethane (Tris)−NaCl buffer after soaking the different specimens treated with the $CaCl_2$ solution as a function of soaking time. The Ca concentration increased up to a soaking time of 1 day, slightly decreased, and then became almost constant for both specimens. The Ca concentration of $VBSO_3$ 2.5Ca after soaking was higher than that of $VBSO_2$ 2.5Ca regardless of soaking time.

Figure 4 shows thin-film X-ray diffraction (TF-XRD) patterns of the copolymer specimens after soaking in SBF for various time intervals. The peaks corresponding to apatite (JCPDS #09-0432) were first observed at 2θ = 26° and 32° after 1 and 14 days in $VBSO_3$ 2.5Ca and $VBSO_2$ 2.5Ca, respectively.

Figure 5A shows scanning electron microscopy (SEM) images of the powdered copolymer specimens without preliminary Ca^{2+} incorporation after soaking in SBF1.5Ca for various time intervals. The surface of $VBSO_3$ 0Ca was still smooth after 7 days, while hemispherical depositions were observed on $VBSO_2$ 0Ca. Figure 5B shows a magnified SEM

DOI: 10.1021/acsomega.8b00694
ACS Omega 2018, 3, 5627−5633

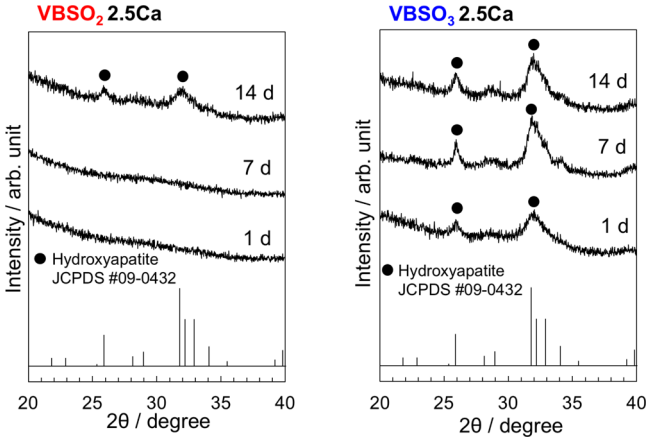

Figure 4. TF-XRD patterns of the different copolymer specimens after soaking in SBF for various time intervals.

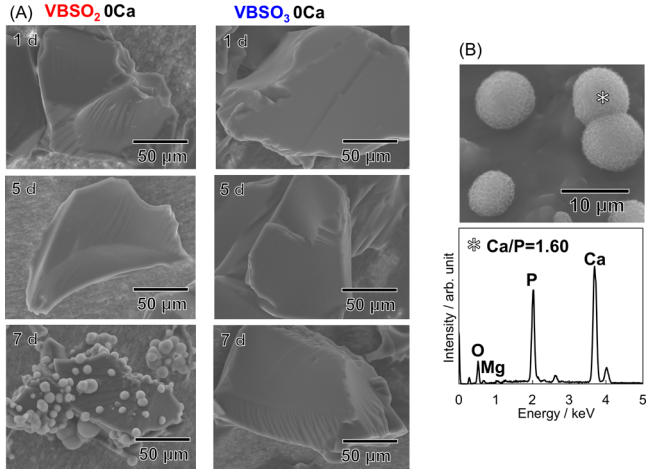

Figure 5. (A) SEM images of the powdered copolymer specimens after soaking in SBF1.5Ca for various time intervals and (B) magnified SEM image of the deposition on $VBSO_2$ 0Ca after 7 days and EDX spectrum of the spot indicated with an asterisk.

image of $VBSO_2$ 0Ca after 7 days and the energy-dispersive X-ray (EDX) spectrum of the depositions detected by point analysis using SEM−EDX. Hemispherical depositions of primary particles with scalelike shapes were observed on its surface. The P, Ca, and Mg peaks were detected in the EDX spectra. The Ca/P molar ratio of the deposition was 1.60. The morphology and the molar ratio were similar to the apatite formed in a simulated body environment.[10]

Figure 6 shows transmission electron microscopy (TEM) images of the surface of powdered specimens after being soaked in SBF1.5Ca for various time intervals. Depositions with a diameter around 20 nm were observed on the surface of $VBSO_2$ 0Ca after 3 days, and the diameter increased to 50−100 nm after 5 days. Fine particles with a diameter of about 20 nm were observed on the surface of $VBSO_3$ 0Ca after 5 days.

Figure 7 shows the change in Ca and P concentrations in SBF1.5Ca after soaking the powdered copolymer specimens for various time intervals. Decreased concentrations of both were observed after soaking both specimens. The concentration decrease was higher for $VBSO_2$ 0Ca than for $VBSO_3$ 0Ca.

Table 1 shows the zeta potential of the powdered copolymer specimens after soaking in the Tris−NaCl buffer and the stability constant of the Ca^{2+} complex composed of the ionized

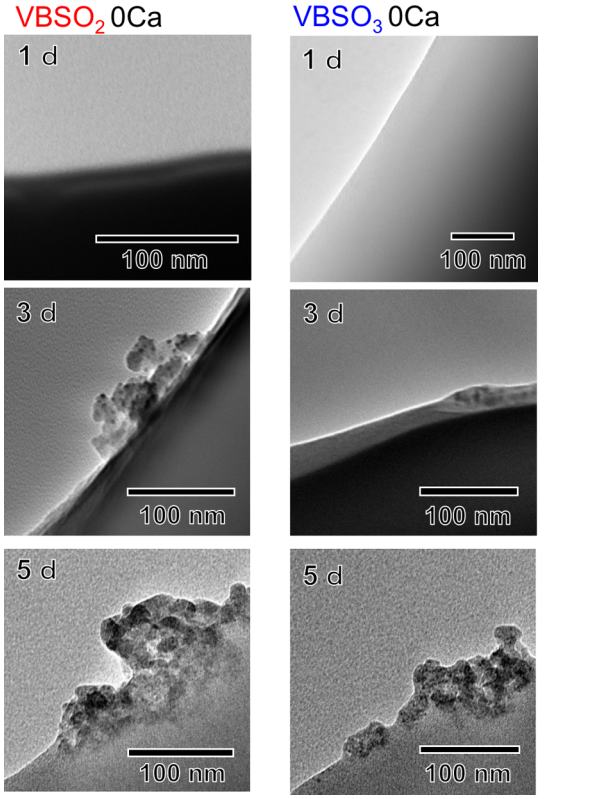

Figure 6. Bright-field TEM images of the powdered copolymer specimens after soaking in SBF1.5Ca for various time intervals.

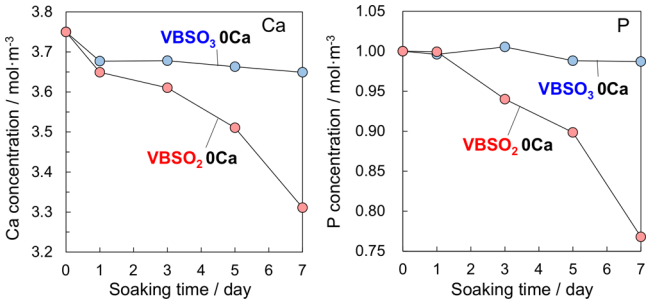

Figure 7. Change in Ca and P concentration in SBF1.5Ca after soaking the powdered copolymer specimens for various time intervals.

Table 1. Zeta Potential of the Powdered Polymer Specimens (n = 3) and Stability Constant of the Complexes Consisting of Each Acidic Functional Group and Ca^{2+} at μ = 0.16

	$VBSO_2$ 0Ca, $-SO_2H$	$VBSO_3$ 0Ca, $-SO_3H$
zeta potential/mV	−16.8 ± 2.3	−18.5 ± 5.4
stability constant log β	1.61	1.31

p-toluenesulfinic acid or *p*-toluenesulfonic acid. $VBSO_2$ 0Ca and $VBSO_3$ 0Ca had nearly equivalent negative potentials at the ion strength of physiological conditions. The stability constant of the *p*-toluenesulfinate−Ca^{2+} complex was higher than that of the *p*-toluenesulfonate−Ca^{2+} complex.

3. DISCUSSION

Copolymers with nearly equivalent amounts of different acidic functional groups were successfully obtained using the same method (Figure 2A). This was confirmed by FT-IR spectra showing that only $VBSO_3$ displayed the O═S═O peak

DOI: 10.1021/acsomega.8b00694
ACS Omega 2018, 3, 5627−5633

characteristic to $-SO_3H$ (Figure 1). The apatite formation in SBF was faster on $VBSO_3$ than on $VBSO_2$ when they were treated with $CaCl_2$ solution (Figure 4). This means that $-SO_3H$ on the copolymers was more effective for apatite formation than $-SO_2H$ with coexistence of Ca^{2+}.

The induction of the apatite formation on a substrate depends on the surface conditions and supersaturation degree with respect to apatite in SBF.[27] The release of Ca^{2+} from the surface is especially effective for increasing the supersaturation degree.[5] $VBSO_3$ 2.5Ca was able to release larger amounts of Ca^{2+} than $VBSO_2$ 2.5Ca (Figure 3), meaning that the former provided more favorable conditions for the apatite formation in SBF. However, the Ca content in $VBSO_3$ 2.5Ca was lower than that in $VBSO_2$ 2.5Ca after soaking in $CaCl_2$ solution (Figure 2B). The Ca^{2+} release from the copolymers into the SBF is expected to be governed by the initial Ca content and its binding with surrounding anionic functional groups. It has been reported that Ca^{2+} release is inhibited by the increased $-SO_3H$ content in the copolymers via formation of a complex such as $(-SO_3^-)_2\cdots Ca^{2+}$.[18]

In this study, the copolymers were composed of functional groups with different structures. The change of Gibbs free energy (ΔG) during the formation of the complex is related to the stability constant of the complex (β) as shown in eq 1

$$\Delta G = -2.303RT \log \beta \quad (1)$$

where R is the gas constant and T is the temperature of the solution. On the basis of the measured stability constant of the Ca^{2+} complex (Table 1), the formation of $(-SO_2^-)_2\cdots Ca^{2+}$ gave a lower negative value of ΔG than $(-SO_3^-)_2\cdots Ca^{2+}$ at the same temperature. The difference in ΔG value indicates that the interaction of $(-SO_2^-)_2\cdots Ca^{2+}$ was thermodynamically more stable than $(-SO_3^-)_2\cdots Ca^{2+}$ under physiological conditions. Thus, it is assumed that the ability of $-SO_3H$ to trap Ca^{2+} in the copolymers is weak, which results in the enhancement of the Ca^{2+} release. Modification with $-SO_3H$ has the advantage of apatite formation on the hybrids.

In contrast, $-SO_2H$ in $VBSO_2$ 0Ca induced the apatite formation faster than $-SO_3H$ in $VBSO_3$ 0Ca under the condition in which Ca^{2+} was not released to keep the supersaturation degree constant with respect to the apatite (Figure 5A,B). This phenomenon is opposite to what happens to the present copolymers modified with Ca^{2+}. Dey et al. observed the mechanism of apatite formation on the monolayer of arachidic acid in SBF using cryo-TEM.[28] They showed that 50−80 nm diameter spherical nodules of amorphous calcium phosphate were formed by the aggregation of the calcium phosphate complex on the monolayer, resulting in conversion to apatite. Habraken et al. determined that the composition of the amorphous phase is $[Ca_2(HPO_4)_3]^{2-}$, which grows into Ca-defected octacalcium phosphate as a precursor of the apatite in the solution.[29] In the present study, both $VBSO_2$ 0Ca and $VBSO_3$ 0Ca also initially formed particles on their surfaces with diameters similar to the above reports (Figure 6). Moreover, Ca and P consumption in SBF1.5Ca within 5 days suggested calcium phosphate formation on $VBSO_2$ 0Ca and $VBSO_3$ 0Ca (Figure 7). Thus, it is assumed that $-SO_2H$ could induce formation of a larger amount of calcium phosphate as a precursor of the apatite at an earlier stage of soaking than $-SO_3H$.

According to previous reports on the heterogeneous nucleation process of apatite, bioactive materials initially adsorb Ca^{2+}, and then phosphate ions on their surface form calcium phosphate in the SBF.[30,31] Yamashita et al. reported that hydroxyapatite subjected to electric poling had a highly negatively charged surface and promoted apatite formation because the amount of adsorbed Ca^{2+} increased on its surface.[32] However, ion−ion interactions with Ca^{2+} were also considered as a factor of the Ca^{2+} adsorption for apatite formation.[9] Judging from the higher rate of decrease in Ca concentration at the initial stage of soaking (Figure 7), it is assumed that $VBSO_2$ 0Ca had a more favorable surface for Ca^{2+} adsorption compared with $VBSO_3$ 0Ca. There was no significant difference in the zeta potential on each specimen (Table 1). Therefore, the different stability constants of the two complexes should be the main factor affecting the apatite-forming ability, although statistical significance remains to be confirmed in the future.

On the basis of the discussion described above, the detailed mechanism of apatite formation on the copolymer in SBF1.5Ca is expected to progress as follows. (1) Chemical interaction of $-SO_3^-\cdots Ca^{2+}$ or $-SO_2^-\cdots Ca^{2+}$ was constructed on the surface of each specimen at initial stage of soaking. (2) HPO_4^{2-} in SBF1.5Ca was adsorbed on the surface because the surface potential increases from negative to positive after the initial adsorption of Ca^{2+}.[30,31] (3) HPO_4^{2-} reacted with the Ca^{2+} bonded to the functional groups to form the spherical particles of amorphous calcium phosphate (Figure 6). (4) The amorphous particles transformed and grew into apatite (Figure 5) because of the consumption of the ions in SBF1.5Ca (Figure 7). Regarding the reaction in the process (3), our previous research suggests that formation of $Ca^{2+}\cdots HPO_4^{2-}$ interaction increases the concentration of the calcium phosphate complexes which aggregate to the $[Ca_2(HPO_4)_3]^{2-}$ cluster on the copolymer.[23] Moreover, Kawai et al. reported that the crystal growth of apatite is governed by the supersaturation degree regardless of the type of anionic functional groups on the surface in a simulated body environment.[27] It means that difference in the chemical structure of functional groups changes the behavior of apatite formation during the process of (1−3) without Ca^{2+} release from the copolymer. Therefore, it is assumed that $-SO_2H$ adsorbed a large amount of Ca^{2+} and accelerated the $Ca^{2+}\cdots HPO_4^{2-}$ formation and the subsequent aggregation, resulting in enhancement of the apatite deposition on $VBSO_2$ 0Ca.

In conclusion, it was found that the apatite formation induced by various sulfur-containing functional groups was significantly altered by the coexistence of Ca^{2+}. Namely, the low stability of $-SO_3^-\cdots Ca^{2+}$ improved the apatite-forming ability of the Ca^{2+}-modified copolymers, although $-SO_3H$ by itself had a lower ability of inducing heterogeneous apatite nucleation than $-SO_2H$. This is because Ca^{2+} released from the $-SO_3^-\cdots Ca^{2+}$ decreased the activation energy for heterogeneous nucleation and increased the rate of crystal growth on the copolymers. It has been reported that apatite growth on the polymer substrate is also related to the supersaturation degree in the simulated body environment.[27]

The Ca^{2+} bound to the material surface can adsorb the proteins, leading to the osteoblast adhesion and osteoconductivity of the titanium.[33,34] In addition, it has been reported that suitable Ca^{2+} concentration in the medium impacts osteoblast differentiation.[35] Consequently, it is expected that the structural differences of these functional groups affect the osteoblast activities and the bone-bonding ability through the state of binding with Ca^{2+}. To confirm this, the behavior of protein adsorption and the activities of the cells on the different hybrids should be investigated.

DOI: 10.1021/acsomega.8b00694
ACS Omega 2018, 3, 5627−5633

4. CONCLUSIONS

The apatite-forming behavior of copolymers modified with $-SO_2H$ or $-SO_3H$ was examined in a simulated body environment. When they were modified with Ca^{2+}, $-SO_3H$ formed apatite on the surface faster than $-SO_2H$. It was assumed that the low stability of $-SO_3^-\cdots Ca^{2+}$ had the advantage of Ca^{2+} release, which promoted both heterogeneous nucleation and crystal growth of the apatite. In contrast, the opposite phenomenon was observed when they were not modified with Ca^{2+}. High stability of the $-SO_2^-\cdots Ca^{2+}$ interaction enhanced the heterogeneous nucleation of the apatite on the copolymers. It was found that the stability of the interaction with Ca^{2+} depended on the structure of these functional groups and was an important factor governing the apatite formation.

5. MATERIALS AND METHODS

5.1. Specimen Preparation. $NaVBSO_2$ (90%, Tokyo Chemical Industry Co. Ltd., Tokyo, Japan) and $NaVBSO_3$ (90%, Sigma-Aldrich Co., Saint Louis, USA) were used to incorporate the $-SO_2H$ and $-SO_3H$ groups, respectively, into the copolymer. A total of 1.0 mmol of $NaVBSO_2$ or $NaVBSO_3$ and 9.0 mmol of HEMA (95%, Wako Pure Chemical Industries Ltd., Osaka, Japan) were dissolved in ultrapure water. Furthermore, 5.0×10^{-4} mol of *N*,*N*′-methylenebisacrylamide (99%, Wako Pure Chemical Industries Ltd.) and 1.5×10^{-5} mol of *N*,*N*,*N*′,*N*′-tetramethylethylenediamine (98%, Wako Pure Chemical Industries Ltd.) and 2,2′-azobis(2-methylpropionamidine)dihydrochloride (95%, Wako Pure Chemical Industries Ltd.) were added. The mixture of these regents was adjusted to a total volume of 10 cm^3 in a volumetric flask. To copolymerize these monomers, 1 cm^3 of the resulting solution was put in a polyethylene cup at 60 °C for 1 day.

The obtained copolymers were cut into ϕ 5 × 1 mm cylinders. They were soaked in 1 $kmol{\cdot}m^{-3}$ HCl solution for 1 day to remove the unreacted reagents and sodium ions, soaked in ultrapure water for 1 day, and then dried in vacuum. The obtained copolymers were then soaked in 30 cm^3 of 0 or 2.5 $mol{\cdot}m^{-3}$ $CaCl_2$ solution at 36.5 °C for 1 day. The copolymers prepared from $NaVBSO_2$ and $NaVBSO_3$ were abbreviated as $VBSO_2$ *X*Ca and $VBSO_3$ *X*Ca, respectively, where *X* indicates the concentration of the $CaCl_2$ solution used. $VBSO_2$ and $VBSO_3$ indicate the specimens without $CaCl_2$ treatment.

5.2. Soaking Specimens in SBF and SBF1.5Ca To Evaluate Apatite-Forming Ability. The cylindrical $VBSO_2$ 2.5Ca and $VBSO_3$ 2.5Ca specimens were soaked in 30 cm^3 of SBF (Na^+ 142.0, K^+ 5.0, Mg^{2+} 1.5, Ca^{2+} 2.5, Cl^- 147.8, HCO_3^- 4.2, HPO_4^{2-} 1.0, SO_4^{2-} 0.5 $mol{\cdot}m^{-3}$, pH 7.40) for various time intervals. In addition, 9 mg of powdered $VBSO_2$ 0Ca and $VBSO_3$ 0Ca specimens was soaked in SBF1.5Ca, which has Ca^{2+} concentration 1.5 times that of the normal SBF[36] with a pH 7.25 at 36.5 °C for various time intervals. The powder was prepared by cooling the bulk specimen using liquid N_2 and pulverizing it with a porcelain mill and agate balls.

SBF and SBF1.5Ca were prepared by dissolution of NaCl, $NaHCO_3$, KCl, $K_2HPO_4{\cdot}3H_2O$, $MgCl_2{\cdot}6H_2O$, $CaCl_2$, and Na_2SO_4 (Nacalai Tesque, Inc., Kyoto, Japan) in ultrapure water in that order. The pH for each resulting solution was adjusted by the addition of 1 $kmol{\cdot}m^{-3}$ HCl solution and Tris (Nacalai Tesque, Inc.).

5.3. Soaking Specimens in Tris−NaCl Buffer To Measure Ca^{2+} Release. The hybrid specimens were soaked in 30 cm^3 of Tris−NaCl buffer (NaCl 142, Tris 50 $mol{\cdot}m^{-3}$, pH 7.40) at 36.5 °C for various time intervals to measure the amount of released Ca^{2+}. The Tris−NaCl buffer was prepared by the addition of NaCl and Tris in ultrapure water, and the pH was adjusted with the addition of 1 $mol{\cdot}m^{-3}$ HCl.

5.4. Specimen Characterization. The chemical structure of the different copolymers was analyzed by FT-IR spectroscopy (FT/IR-6100, JASCO Co., Tokyo, Japan) using an attenuated total reflectance method. The content of acidic functional groups in the specimens was measured by neutralizing titration. A 30 cm^3 of 0.16 $kmol{\cdot}m^{-3}$ NaCl solution with specimens soaked without Ca^{2+} was titrated with 10.0 $mol{\cdot}m^{-3}$ of the NaOH solution. The point of neutralization was determined by the change in pH of the solution measured by a pH meter (F-23IIC, Horiba Ltd., Kyoto, Japan). To determine the Ca content in the specimens, the decrease in Ca concentration in the $CaCl_2$ solution after soaking of specimens was measured using inductively coupled plasma atomic emission spectrometry (ICP−AES; ICPE-9820, SHIMADZU Co., Kyoto, Japan).

After the specimens were soaked in SBF or SBF1.5Ca, they were analyzed by TF-XRD (MXP3V, Mac Science Co., Yokohama, Japan) and EDX (EMAX Energy, Horiba Ltd) equipped with a scanning electron microscope (S-3500N, Hitachi Co., Tokyo, Japan). In the TF-XRD analysis, the incident X-ray (monochromatic Cu Kα radiation) was fixed at 1° relative to the specimen surface with a scan rate of $0.02°{\cdot}s^{-1}$. After the immersion in SBF1.5Ca, the powder specimens were deposited onto a Cu grid with 250 mesh (ELS-C10, Okenshoji Co., Ltd., Tokyo, Japan). Ultrapure water was then added several times to remove the SBF1.5Ca from the grid. The surface was then observed with a transmission electron microscope (JEM-3010, JEOL Ltd., Tokyo, Japan).

The surface zeta potential of the powdered copolymer specimens was measured by the zeta potential analyzer (ELS-Z, Otsuka Electronic Co., Osaka, Japan). The Tris−NaCl buffer with soaked specimens was injected into the quartz cell, and the electrophilic mobility was measured by the laser Doppler method to calculate the zeta potential. The Ca concentration in the Tris−NaCl buffer and Ca and P concentrations in the specimens soaked in SBF1.5Ca for various time intervals were measured using ICP−AES.

5.5. Determination of the Stability Constant of the Complexes. The stability constant of the complexes, which consisted of Ca^{2+} and the ligand of ionized *p*-toluenesulfinic acid or *p*-toluenesulfonic acid, was determined to compare the thermodynamic stability of the interaction between Ca^{2+} and each acid group. A 3.0−4.2 mmol of sodium *p*-toluenesulfinate (98%, Tokyo Chemical Industry Co., Ltd.) or *p*-toluenesulfonic acid monohydrate (99%, Wako Pure Chemical Industries Ltd.) was dissolved in 30 cm^3 of $mol{\cdot}m^{-3}$ $CaCl_2$ solution. The ion strength and pH were adjusted to 0.16 and 6.4−6.7, respectively, by the addition of NaCl and Tris. The free Ca^{2+} concentration in the solution was measured using a Ca^{2+}-ion-selective electrode (6583-10C, Horiba Ltd.). The stability constant, β, of the Ca^{2+} complex was calculated with eq 2

$$\beta = \frac{[L_2\cdots Ca^{2+}]}{[L]^2[Ca^{2+}]} = \frac{[Ca^{2+}]_{total} - [Ca^{2+}]}{([L]_{total} - 2\{[Ca^{2+}]_{total} - [Ca^{2+}]_{free}\})^2[Ca^{2+}]} \quad (2)$$

DOI: 10.1021/acsomega.8b00694
ACS Omega 2018, 3, 5627−5633

where $[L_2\cdots Ca^{2+}]$, [L], and $[Ca^{2+}]$ are molar concentrations of the complex, free ligand, and free Ca^{2+}, respectively. $[L]_{total}$ and $[Ca^{2+}]_{total}$ are the total concentration of ligand and Ca^{2+} in the solution, respectively.

AUTHOR INFORMATION

Corresponding Author

*E-mail: tmiya@life.kyutech.ac.jp. Fax: +81-93-695-6025.

ORCID

Toshiki Miyazaki: 0000-0001-5642-0096

Notes

The authors declare no competing financial interest.

ACKNOWLEDGMENTS

This study was partially supported by a Grant-in-Aid for JSPS Research Fellow, grant number 17J02000. We thank Melissa Gibbons, PhD, from Edanz Group (www.edanzediting.com/ac) for editing a draft of this manuscript.

REFERENCES

(1) Hench, L. L. Bioceramics. *J. Am. Ceram. Soc.* **1998**, *81*, 1705−1728.

(2) Kokubo, T.; Kim, H.-M.; Kawashita, M. Novel Bioactive Materials with Different Mechanical Properties. *Biomaterials* **2003**, *24*, 2161−2175.

(3) Jarcho, M.; Bolen, C. H.; Thomas, M. B.; Bobick, J.; Kay, J. F.; Doremus, R. H. Hydroxyapatite Synthesis and Characterization in Dense Polycrystalline Forms. *J. Mater. Sci.* **1976**, *11*, 2027−2035.

(4) Jacho, M.; Kay, J. F.; Gumaer, R. H.; Drobeck, H. P. Tissue, Cellular and Subcellular Events at Bone-ceramics Hydroxyapatite Interface. *J. Bioeng.* **1977**, *1*, 79−92.

(5) Ohtsuki, C.; Kokubo, T.; Yamamuro, T. Mechanism of Apatite Formation on $CaO\text{-}SiO_2\text{-}P_2O_5$ Glass in a Simulated Body Fluid. *J. Non-Cryst. Solids* **1992**, *143*, 84−92.

(6) Li, P.; Ohtsuki, C.; Kokubo, T.; Nakanishi, K.; Soga, N.; de Groot, K. The Role of Hydrated Silica, Titania, and Alumina in Inducing Apatite on Implants. *J. Biomed. Mater. Res.* **1995**, *28*, 7−15.

(7) Uchida, M.; Kim, H.-M.; Kokubo, T.; Nakamura, T. Bonelike Apatite Formation Induced on Zirconia Gel in Simulated Body Fluid and Its Modified Solution. *J. Am. Ceram. Soc.* **2004**, *84*, 2041−2044.

(8) Miyazaki, T.; Kim, H.-M.; Kokubo, T.; Kato, T.; Nakamura, T. Induction and Acceleration of Bonelike Apatite Formation on Tantalum Oxide Gel in Simulated Body Fluid. *J. Sol-Gel Sci. Technol.* **2001**, *21*, 83−88.

(9) Tanahashi, M.; Matsuda, T. Surface Functional Group Dependence on Apatite Formation on Self-assembled Monolayers in a Simulated Body Fluid. *J. Biomed. Mater. Res.* **1997**, *34*, 305−315.

(10) Kawai, T.; Ohtsuki, C.; Kamitakahara, M.; Miyazaki, T.; Tanihara, M.; Sakaguchi, Y.; Konagaya, S. Coating of an Apatite Layer on Polyamide Films Containing Sulfonic Groups by a Biomimetic Process. *Biomaterials* **2004**, *25*, 4529−4534.

(11) Cho, S.-B.; Nakanishi, K.; Kokubo, T.; Soga, N.; Ohtsuki, C.; Nakamura, T.; Kitsugi, T.; Yamamuro, T. Dependence of Apatite Formation on Silica Gel on Its Structure: Effect of Heat Treatment. *J. Am. Ceram. Soc.* **1995**, *78*, 1769−1774.

(12) Kokubo, T.; Takadama, H. How Useful is SBF in Predicting in vivo Bone Bioactivity? *Biomaterials* **2006**, *27*, 2907−2915.

(13) Kim, H.-M.; Miyaji, F.; Kokubo, T.; Nakamura, M. Effect of Heat Treatment on Apatite Forming Ability of Ti Metal Induced by alkali treatment. *J. Mater. Sci.: Mater. Med.* **1997**, *8*, 341−343.

(14) Osaka, A.; Tsuru, K.; Hayakawa, S. Titania Derived form Combined Chemical and Thermal Treatment of Titanium: in vitro Apatite Forming Ability. *Phosphorus Res. Bull.* **2004**, *17*, 130−141.

(15) Tsuru, K.; Ohtsuki, C.; Osaka, A.; Iwamoto, T.; Mackenzie, J. D. Bioactivity of Sol-gel Derived Organically Modified Silicate: Part 1: in vitro Examination. *J. Mater. Sci.: Mater. Med.* **1997**, *8*, 157−161.

(16) Kamitakahara, M.; Kawashita, M.; Miyata, N.; Kokubo, T.; Nakamura, T. Preparation of Bioactive Flexible Poly(tetramethylene oxide)(PTMO)-CaO-Ta_2O_5 Hybrids. *J. Mater. Sci.: Mater. Med.* **2007**, *18*, 1117−1124.

(17) Miyazaki, T.; Matsunami, C.; Shirosaki, Y. Bioactive Carbon-PEEK Composites Prepared by Chemical Surface Treatment. *Mater. Sci. Eng., C* **2017**, *70*, 71−75.

(18) Miyazaki, T.; Imamura, M.; Ishida, E.; Ashizuka, M.; Ohtsuki, C. Apatite Formation Abilities and Mechanical Properties of Hydroxyethylmethacrylate-based Organic-inorganic Hybrids Incorporated with Sulfonic Groups and Calcium Ions. *J. Mater. Sci.: Mater. Med.* **2009**, *20*, 157−161.

(19) Chaterji, S.; Gemeinhart, R. A. Enhanced Osteoblast-like Cell Adhesion and Proliferation Using Sulfonate-bearing Polymeric Scaffold. *J. Biomed. Mater. Res., Part A* **2007**, *83*, 990−998.

(20) López-Pérez, P. M.; da Silva, R. M. P.; Sousa, R. A.; Pashkuleva, I.; Reis, R. L. Plasma-Induced Polymerization as a Tool for Surface Functionalization of Polymer Scaffolds for Bone Tissue Engineering: An in vitro Study. *Acta Biomater.* **2010**, *6*, 3704−3712.

(21) Hamai, R.; Shirosaki, Y.; Miyazaki, T. Apatite Formation on A Hydrogel Containing Sulfinic Acid Group under Physiological Conditions. *J. Biomed. Mater. Res., Part B* **2017**, *105*, 1924−1929.

(22) Perrin, D. D.; Dempesy, B.; Serjeant, E. P. Molecular Factor That Modify pK_a Value. In *pK_a Prediction for Organic Acid and Bases*; Perrin, D. D., Dempesy, B., Serjeant, E. P., Eds.; Springer: Berlin, 1981; pp 12−20.

(23) Hamai, R.; Maeda, H.; Sawai, H.; Shirosaki, Y.; Kasuga, T.; Miyazaki, T. Structural Effects of Phosphate Groups on Apatite Formation in Copolymer Modified with Ca^{2+} in a Simulated Body Fluid. *J. Mater. Chem. B* **2018**, *6*, 174−182.

(24) Ferreira, L.; Vidal, M. M.; Gil, M. H. Evaluation of Poly(2-hydroxyethyl methacrylate) Gels as Drug Delivery System at Different pH Value. *Int. J. Pharm.* **2000**, *194*, 169−180.

(25) Halm, C.; Evarts, J.; Kurth, M. J. A New Attachment/Cleavage Strategy: Polymer-Bound Allylic Sulfones in a Solid-phase Route to Trisubstituted Olefins. *Tetrahedron Lett.* **1997**, *38*, 7709−7712.

(26) Chiono, V.; Carmagnola, I.; Gentile, P.; Boccafoschi, F.; Tonda-Turo, C.; Ballarini, M.; Georgieva, V.; Georgiev, G.; Ciardelli, G. Layer-by-layer Coating of Photoactive Polymers for Biomedical Applications. *Surf. Coat. Technol.* **2012**, *206*, 2446−2453.

(27) Kawai, T.; Ohtsuki, C.; Kamitakahara, M.; Tanihara, M.; Miyazaki, T.; Sakaguchi, Y.; Konagaya, S. A Comparative Study of Apatite Deposition on Polyamide Films Containing Different Functional Groups under a Biomimetic Condition. *J. Ceram. Soc. Jpn.* **2005**, *113*, 588−592.

(28) Dey, A.; Bomans, P. H. H.; Müller, F. A.; Will, J.; Frederik, P. M.; de With, G.; Sommerdijk, N. A. J. M. The Role of Prenucleation Clusters in Surface-induced Calcium Phosphate Crystallization. *Nat. Mater.* **2010**, *9*, 1010−1014.

(29) Habraken, W. J. E. M.; Tao, J.; Brylka, L. J.; Friendrich, H.; Bertinetti, L.; Schenk, A. S.; Verch, A.; Dmitrovic, V.; Bomans, P. H. H.; Frederik, P. M.; Laven, J.; van der Schoot, P.; Aichmayer, B.; de With, G.; DeYoreo, J. J.; Sommerdijk, N. A. J. M. Ion-association Complexes unite Classical and Non-classical Theories for The Biomimetic Nucleation of Calcium Phosphate. *Nat. Commun.* **2013**, *4*, 1507.

(30) Takadama, H.; Kim, H.-M.; Kokubo, T.; Nakamura, T. An X-ray Photoelectron Spectroscopy Study of The Process of Apatite Formation on Bioactive Titanium Metal. *J. Biomed. Mater. Res.* **2001**, *55*, 185−193.

(31) Kim, H.-M.; Himeno, T.; Kokubo, T.; Nakamura, T. Process and Kinetics of Bonelike Apatite Formation on sintered Hydroxyapatite in a Simulated Body Fluid. *Biomaterials* **2005**, *26*, 4366−4373.

(32) Yamashita, K.; Oikawa, N.; Umegaki, T. Acceleration and Deceleration of Bone-like Crystal Growth on Ceramic Hydroxyapatite by Electric Poling. *Chem. Mater.* **1996**, *8*, 2697−2700.

(33) Feng, B.; Weng, J.; Yang, B. C.; Qu, S. X.; Zhang, X. D. Characterization of titanium surface with calcium and phosphate and osteoblast adhesion. *Biomaterials* **2004**, *25*, 3421−3428.

DOI: 10.1021/acsomega.8b00694
ACS Omega 2018, 3, 5627−5633

(34) Zhang, L.; Ayukawa, Y.; LeGeros, R. Z.; Matsuya, S.; Koyano, K.; Ishikawa, K. Tissue-response to Calcium-bonded Titanium Surface. *J. Biomed. Mater. Res., Part A* **2010**, *95*, 33−39.
(35) Maeno, S.; Niki, Y.; Matsumoto, H.; Morioka, H.; Yatabe, T.; Funayama, A.; Toyama, Y.; Taguchi, T.; Tanaka, J. The Effect of Calcium Ion Concentration on Osteoblast Viability, Proliferation and Differentiation in Monolayer and 3D culture. *Biomaterials* **2005**, *26*, 4847−4855.
(36) Cho, S.-B.; Miyaji, F.; Kokubo, T.; Nakanishi, K.; Soga, N.; Nakamura, T. Apatite Formation on Various Silica Gels in a Simulated Body Fluid Containing Excessive Calcium Ion. *J. Ceram. Soc. Jpn.* **1996**, *104*, 399−404.

DOI: 10.1021/acsomega.8b00694
ACS Omega 2018, 3, 5627−5633